

HETE-2 Observation of two gamma-ray bursts at $z > 3$

J.-L. Atteia,³ N. Kawai,^{4,5} R. Vanderspek,¹ G. Pizzichini,¹⁶ G. R. Ricker,¹ C. Barraud,³
M. Boer,¹⁸ J. Braga,¹⁴ N. Butler,¹ T. Cline,¹³ G. B. Crew,¹ J.-P. Dezalay,¹¹
T. Q. Donaghy,² J. Doty,¹ E. E. Fenimore,¹⁰ M. Galassi,¹⁰ C. Graziani,² K. Hurley,⁶
J. G. Jernigan,⁶ D. Q. Lamb,² A. Levine,¹ R. Manchanda,¹⁵ F. Martel,¹ M. Matsuoka,⁸
E. Morgan,¹ Y. Nakagawa,⁹ J.-F. Olive,¹¹ G. Prigozhin,¹ T. Sakamoto,^{4,5,13} R. Sato,⁴
Y. Shirasaki,^{5,7} M. Suzuki,⁴ K. Takagishi,¹⁷ T. Tamagawa,⁵ K. Torii,¹⁹ J. Villasenor,¹
S. E. Woosley,¹² M. Yamauchi,¹⁷ and A. Yoshida^{5,9}

ABSTRACT

GRB 020124 and GRB 030323 constitute half the sample of gamma-ray bursts with a measured redshift greater than 3. This paper presents the temporal and spectral properties of these two gamma-ray bursts detected and localized with

¹Center for Space Research, Massachusetts Institute of Technology, 70 Vassar Street, Cambridge, MA, 02139.

²Department of Astronomy and Astrophysics, University of Chicago, 5640 South Ellis Avenue, Chicago, IL 60637.

³Laboratoire d’Astrophysique, Observatoire Midi-Pyrénées, 14 Ave. E. Belin, 31400 Toulouse, France.

⁴Department of Physics, Tokyo Institute of Technology, 2-12-1 Ookayama, Meguro-ku, Tokyo 152-8551, Japan.

⁵RIKEN (Institute of Physical and Chemical Research), 2-1 Hirosawa, Wako, Saitama 351-0198, Japan.

⁶University of California at Berkeley, Space Sciences Laboratory, Berkeley, CA, 94720-7450.

⁷National Astronomical Observatory, Osawa 2-21-1, Mitaka, Tokyo 181-8588 Japan.

⁸Tsukuba Space Center, National Space Development Agency of Japan, Tsukuba, Ibaraki, 305-8505, Japan.

⁹Department of Physics, Aoyama Gakuin University, Chitosedai 6-16-1 Setagaya-ku, Tokyo 157-8572, Japan.

¹⁰Los Alamos National Laboratory, P.O. Box 1663, Los Alamos, NM, 87545.

¹¹Centre d’Etude Spatiale des Rayonnements, Observatoire Midi-Pyrénées, 9 Ave. du Colonel Roche, 31028 Toulouse Cedex 4, France.

¹²Department of Astronomy and Astrophysics, University of California at Santa Cruz, 477 Clark Kerr Hall, Santa Cruz, CA 95064.

¹³NASA Goddard Space Flight Center, Greenbelt, MD, 20771.

¹⁴Instituto Nacional de Pesquisas Espaciais, Avenida Dos Astronautas 1758, São José dos Campos 12227-010, Brazil.

¹⁵Department of Astronomy and Astrophysics, Tata Institute of Fundamental Research, Homi Bhabha Road, Mumbai, 400 005, India.

¹⁶INAF/IASF Sezione di Bologna, via Piero Gobetti 101, 40129 Bologna, Italy.

¹⁷Faculty of engineering, Miyazaki University, Gakuen Kibanadai Nishi, Miyazaki 889-2192, Japan.

¹⁸Observatoire de Haute Provence, 04870 St. Michel l’Observatoire, France.

¹⁹Department of Earth and Space Science, Graduate School of Science, Osaka University, 1-1 Machikaneyama, Toyonaka, Osaka 560-0043, Japan

HETE-2. While they have nearly identical redshifts ($z=3.20$ for GRB 020124, and $z=3.37$ for GRB 030323), these two GRBs span about an order of magnitude in fluence, thus sampling distinct regions of the GRB luminosity function. The properties of these two bursts are compared with those of the bulk of the GRB population detected by HETE-2. We also discuss the energetics of GRB 020124 and GRB 030323 and show that they are compatible with the E_p - E_{iso} relation discovered by Amati et al. (2002). Finally, we compute the maximum redshifts at which these bursts could have been detected by HETE-2 and we address various issues connected with the detection and localization of high- z GRBs.

Subject headings: gamma rays: bursts (GRB 020124, GRB 030323)

1. Introduction

High redshift gamma-ray bursts (GRBs) may become useful beacons for the study of the young universe. Gamma-ray bursts are expected to be visible out to very large redshifts ($z=10$ - 20 , Lamb & Reichart 2000), if indeed they are generated there, and offer the possibility to probe the interstellar medium along the line of sight and to address important cosmological issues like the evolution of the star formation rate.

Before one can undertake such studies, however, it is important to understand the intrinsic properties of gamma-ray bursts at high redshift. There are only four GRBs with a measured redshift larger than $z=3$: GRB 971214 at $z=3.42$ (Kulkarni et al. 1998), which was localized by BeppoSAX; GRB 000131 at $z=4.5$ (Andersen et al. 2000), which was localized with the IPN; and GRB 020124 at $z=3.20$ (Hjorth et al. 2003) and GRB 030323 at $z=3.37$ (Vreeswijk et al. 2004), which were localized by HETE-2.

This paper describes the HETE-2 observations of GRB 020124 and GRB 030323. After a quick summary of the localization history of these bursts (section 2), we present their spectral and temporal properties in section 3 and compare them with those of the bulk of the GRB population. Their energetics are discussed in section 4, where it is noted that GRB 030323 is the first GRB detected at large redshift which does not belong to the bright end of the GRB luminosity distribution. In this section we also show that HETE-2 could have detected and localized GRB 020124 at a redshift of $z=6.4$ at least, and we discuss some necessary conditions for the detection of soft, faint GRBs at high redshift. Section 5 looks into the observations of the afterglows and host galaxies of these bursts.

2. Detection, localization, and optical afterglow identification

2.1. GRB 020124

On 2002 January 24, at 10:41:15.15 UT (38475.15 SOD), the High Energy Transient Explorer satellite HETE-2 (hereafter HETE) detected GRB 020124, a moderately bright GRB. No flight localization was issued by the satellite, but the analysis of data on the ground resulted in a coarse localization distributed to the GCN¹ 1.4 hours after the GRB, and in a refined position distributed to the GCN 10.7 hours after the GRB (Ricker et al. 2002). The refined position was a circle of radius 12', centered at RA = 09h 32m 49s, Dec = -11° 27' 35" (J2000). The optical afterglow was reported 28 hours after the GRB, (in data taken 13.5 hours after the GRB) at the position: RA = 09h 32m 50.8s, Dec = -11° 31' 11", well within the refined error box (Price et al. 2002). An IPN annulus was also obtained for this burst, which was fully consistent with the WXM error box (Hurley et al. 2002). Fig. 1a shows the projection of the WXM error box on the sky, the IPN annulus, and the position of the optical afterglow. At the time of its identification, the afterglow had a magnitude R=18.5 (Price et al. 2002). Details of the identification of the optical afterglow and its evolution can be found in Berger et al. (2002). The afterglow spectrum recorded with ISAAC on the VLT-Antu is analysed in Hjorth et al. (2003), who report a redshift $z=3.198$.

2.2. GRB 030323

On 2003 March 23, at 21:56:57.60 UT (79017.60 SOD), HETE detected GRB 030323, a faint GRB. As for GRB 020124 no flight localization was issued by the satellite, but the analysis of data on the ground resulted in a WXM localization distributed to the GCN 5.0 hours after the GRB, and in an SXC localization distributed to the GCN 7.5 hours after the GRB (Graziani et al. 2003). The WXM position was a circle of radius 18', centered at RA = 11h 06m 54s, Dec = -21° 51' 00" (J2000). The SXC position was a trapezoid with an area of 71 arcmin, fully included within the WXM error box. The center of the SXC error box was RA = 11h 06m 06s, Dec = -21° 54' 20" (J2000). The optical afterglow was reported 22 hours after the GRB, (in data taken 9.6 hours after the GRB), at the position: RA = 11h 06m 09.38s, Dec = -21° 46' 13.3" , close to the boundary of the SXC error box, but within it (Gilmore et al. 2003). Fig. 1b shows the projection of the WXM and SXC error boxes on the sky, and the position of the optical afterglow. At the time of its identification, the afterglow

¹Gamma-Ray Burst Coordinate Network, see <http://gcn.gsfc.nasa.gov/>

had a magnitude $R_c=18.7$ (Gilmore et al. 2003). A temporal and spectral analysis of the optical afterglow can be found in Vreeswijk et al. (2004), who report a redshift $z=3.372$.

3. The prompt emission

3.1. Light curves and temporal properties

The light curves of GRB 020124 and GRB 030323 are displayed in Fig. 2. GRB 020124 and GRB 030323 belong to the class of long GRBs with durations $T_{90} = 49.4 \pm 1.3$ sec (GRB 020124), and $T_{90} = 15.0 \pm 2.6$ sec (GRB 030323) in the energy range 6-400 keV. Table 1 gives the durations of these two bursts, and their one sigma errors, in various energy bands. In the FREGATE data, GRB 020124 exhibits little duration shortening with the energy with T_{90} (resp. T_{50}) varying from 51.4 ± 1.4 sec (resp. 26.0 ± 2.7 sec) in the energy band 6-15 keV to 43.0 ± 6.1 sec (resp. 19.2 ± 1.8 sec) in the energy range 85-400 keV. The situation is more confusing in the WXM 2–25 keV energy band (T_{90} and T_{50} seem to follow distinct trends), possibly due to the lower signal to noise ratio of the burst in this instrument. The light curve of GRB 020124 appears very spiky: at least 9 individual spikes can be identified in it.

GRB 030323 is significantly fainter than GRB 020124, and we could only divide the energy range into two subranges : in 6-30 keV we measure $T_{90} = 12.8 \pm 2.5$ sec and $T_{50} = 6.6 \pm 1.5$ sec, and in 30-400 keV we measure $T_{90} = 12.2 \pm 3.6$ sec and $T_{50} = 5.2 \pm 1.6$ sec. With only two energy bands, it is difficult to say whether GRB 030323 exhibits significant duration shortening with energy.

3.2. Spectra

In this section we investigate the average spectral properties of GRB 020124 and GRB 030323. The joint WXM+FREGATE spectra have been fit with a powerlaw times exponential model (PLE), $n(E) \propto E^{-\alpha} \exp(-E/e_0^{\text{obs}})$, and with a Band function (GRBM), which satisfactorily fits most GRB spectra (Band et al. 1993).² This parametrization allows us to compare these bursts with the GRBs detected by BATSE (Band et al. 1993; Preece et al. 2000), BeppoSAX (Frontera et al. 2000; Amati et al. 2002), and HETE (Barraud et al. 2003).

²In this paper we use capital letters for intrinsic spectral parameters (at the source), and lower case letters for the observed spectral parameters.

Sakamoto et al. 2004b). The spectral parameters for the burst-averaged spectra of GRB 020124 and GRB 030323 are given in Table 2. The emission properties of GRB 020124 and GRB 030323 are given in Table 3. Emission properties depend on the model used in the spectral analysis. In Table 3 we report the numbers given in Sakamoto et al. (2004b), which are based on a PLE fit for GRB 020124 and on a simple powerlaw fit for GRB 030323. It should be noted that a spectral analysis based on the best fit Band function (given in Table 2) gives emission parameters which differ by less than 10% from the values given in Table 3. The discussion in section 4, which requires the measure of ‘bolometric’ fluences is based on the best fit Band functions given in Table 2.

3.2.1. GRB 020124

With a fluence of 8.1×10^{-6} erg cm $^{-2}$ in the energy range 2 - 400 keV, GRB 020124 belongs to the brightest third of HETE GRBs. Its ‘softness’³ is 0.32, placing it at the boundary between GRBs and X-Ray Rich GRBs. The peak energy, e_p^{obs} , is relatively well constrained to be about 90 keV. The difference between this value and the value of 133 keV quoted in Barraud et al. (2003) is due to the inclusion of the WXM data covering the range 2-25 keV in this refined analysis.

3.2.2. GRB 030323

With a fluence of 1.2×10^{-6} erg cm $^{-2}$ in the energy range 2 - 400 keV, GRB 030323 belongs to the faintest 20% of HETE GRBs. Its ‘softness’ is 0.38, making it an X-Ray Rich GRB. The e_p^{obs} value of ~ 60 keV is not well constrained and could be as low as 20 keV or as high as 200 keV.

4. Distance and energetics

Knowing the redshifts of GRB 020124 and GRB 030323 allows us to compute their *intrinsic* spectral parameters: E_p , the peak energy of the $\nu F\nu$ spectrum; E_{iso} , the isotropic-equivalent radiated energy (in the energy range 1-10000 keV), and N_γ the isotropic-equivalent

³Following (Sakamoto et al. 2004a), we define the softness as the ratio S_x/S_γ , where S_x is the fluence in the range 2-30 keV, and S_γ is the fluence in the range 30-400 keV. Using this definition X-Ray Flashes have a softness greater than 1 and X-Ray Rich GRBs have a softness in the range 0.33 to 1.

photon number in the same energy range. In the following we adopt a flat cosmology with $\Omega_m = 0.3$, $\Omega_\Lambda = 0.7$, and $h_0 = 0.65$. For GRB 020124, we get $E_p = 390_{-120}^{+70}$ keV, $E_{\text{iso}} = 25 \pm 6 \times 10^{52}$ erg, and $N_\gamma = 34_{-10}^{+20} \times 10^{58}$ photons. For GRB 030323, we get $E_p = 270_{-180}^{+600}$ keV, $E_{\text{iso}} = 3.2 \pm 1 \times 10^{52}$ erg, and $N_\gamma = 5.4_{-2.5}^{+6} \times 10^{58}$ photons.

We note that GRB 020124 is intrinsically bright, similar to GRB 971214, which had $E_{\text{iso}} = 3 \times 10^{53}$ erg (Kulkarni et al. 1998; Dal Fiume et al. 2000; Amati et al. 2002); and GRB 000131 which had $E_{\text{iso}} = 11 \times 10^{53}$ erg (Andersen et al. 2000). The isotropic-equivalent energy of GRB 030323 is however about an order of magnitude fainter, a fact that demonstrates the ability of HETE to detect and localize high-redshift GRBs that are not at the bright end of the GRB luminosity function.

We have checked whether GRB 020124 and GRB 030323 are compatible with the empirical $E_{\text{iso}} - E_p$ relation discovered by Amati et al. (2002), which can be expressed as $E_{\text{iso}}^{0.5} / E_p \sim 1$ (where E_{iso} is measured in units of 10^{50} erg and E_p in keV; see also Lamb et al. 2005). This is indeed the case with $E_{\text{iso}}^{0.5} / E_p = 1.3$ for GRB 020124. For GRB 030323 the E_p of GRB 030323 is not well determined and we cannot draw any conclusion based on this burst (although for the sake of completeness we should mention that the best fit values give $E_{\text{iso}}^{0.5} / E_p = 0.65$). The spectral parameters of GRB 020124 are well determined, and the fact that this burst follows the $E_{\text{iso}} - E_p$ relation closely could indicate that this relation has little or no evolution with the redshift.

4.1. The maximum distances at which GRB 020124 and GRB 030323 could be localized

Fig. 4 shows the position of GRB 020124 and GRB 030323 (the two large triangles, GRB 020124 is the rightmost large triangle) in a fluence-softness diagram, among the population of GRBs detected with HETE (Barraud et al. 2004). This figure also shows the positions that these bursts would have in the same diagram if they had occurred at redshifts 1, 2, 5, 10, and 20. The tracks of GRB 020124 and GRB 030323 in the figure are computed by taking into account the spectral redshift of the bursts, and assuming that we can measure the total fluence, even when the burst is at a high redshift. From this figure we can see that, at redshift 1, GRB 020124 would have been one of the brightest GRBs detected by HETE, while GRB 030323 would have been in the middle of the fluence distribution. Regarding their hardness, we note that at a redshift of unity, GRB 020124 and GRB 030323 would both have been unambiguously classified as 'GRBs', rather than XRR-GRBs or XRFs.

Figure 4 can also be used to discuss the maximum redshift at which HETE could have

detected GRB 020124 and GRB 030323. Based on this figure, we see that GRB 030323 is very close to the boundary of the GRB population detected and localized with HETE. In contrast, the fluence of GRB 020124 appears to remain well within the distribution of localized GRBs up to redshift $z \sim 15$. In reality, the fluence is not the best intensity indicator for GRB *detection* because the trigger algorithm is essentially based on the search for excess counts in short time intervals. In order to assess more precisely the maximum redshift at which HETE could have detected GRB 020124, we have performed a detailed analysis including the following steps:

- Compute the trigger threshold (number of counts) of FREGATE at the time of GRB 020124, on the 1.3 sec and on the 5.2 sec trigger timescales.
- Estimate the signal to noise ratio of GRB 020124 for its detection by FREGATE.
- Determine the redshift at which the counts from GRB 020124 would reach the trigger threshold of FREGATE, taking into account the effects of the distance, of the time dilation and of the spectral redshift of the photons.

This analysis shows that a burst 3.2 times fainter than GRB 020124 would have triggered FREGATE in the 7-30 keV energy range in a time window of 5.2 sec. We thus conclude that GRB 020124 could have been detected by FREGATE up to a redshift $z=6.4$. The trigger scheme of HETE includes many more trigger possibilities than the simple trigger palette of FREGATE, especially some using longer timescales for triggering. It is thus reasonable to assume that GRB 020124 could have been detected by HETE up to redshift 7-8. At this redshift HETE could have localized GRB 020124 because its localization capabilities are more dependent on the fluence of the burst than on its peak flux, and because the fluence decreases more slowly than the peak flux with the redshift. This is confirmed by figure 4 which shows that, at a redshift $z=8$, the fluence and the softness of GRB 020124 would have been comparable with the fluences and softness of many GRBs localized by HETE.

We finally note that, at redshifts higher than 10, the fluence of GRB 020124 remains comparable with the fluence of many GRBs detected and localized with HETE while its peak flux is well below the detection threshold. A consequence of this fact is that a mission can greatly improve its ability to detect high- z GRBs if it is able to localize long, faint, soft transients. This is not the case for BeppoSAX and HETE-2 whose detection strategy is mainly based on the search for count excesses on relatively short timescales. A strategy based on the search for long, soft transients appearing in the *image* of the sky, as is the case for SWIFT-BAT, appears more promising for detecting high- z GRBs.

5. Afterglows and hosts of GRB 020124 and GRB 030323

The discussion in this section is mainly based on the information that has been published in papers on the afterglows and hosts of the four GRBs with a measured redshift greater than 3: GRB 971214 (Halpern et al. 1998; Kulkarni et al. 1998; Dal Fiume et al. 2000), GRB 000131 (Andersen et al. 2000), GRB 020124 (Berger et al. 2002; Hjorth et al. 2003), and GRB 030323 (Vreeswijk et al. 2004).

5.0.1. Spectroscopy of the afterglows

Thanks to fast localizations by HETE, the afterglows of GRBs 020124 and 030323 were observed soon after the burst, while they were still bright. The identification of the afterglow of GRB 020124 is due to Price et al. (2002) in data taken 13.5 hours after the burst, but the first observation took place only two hours after the trigger and caught the afterglow at a magnitude $R=18.5$ (Torii et al. 2002). The identification of the afterglow of GRB 030323 is due to Gilmore et al. (2003) in data taken 9.5 hours after the burst. The afterglow was first observed with ROTSE III, when it had a magnitude $R=18.4$, 6 hours after the burst. This contrasts with the afterglows of GRB 971214, and GRB 000131, which were identified when they had magnitudes $R=22.1$, and $R=23.3$, respectively. These quick detections allowed for spectroscopy of the afterglows while they were still moderately bright ($R=24$ for GRB 020124 and $R=21.5$ for GRB 030323). The spectroscopic observations of GRB 020124 and GRB 030323 resulted in high quality spectra and in the detection of strong Absorption Line Systems (ALS) in the afterglows of both GRBs (Hjorth et al. 2003; Vreeswijk et al. 2004).

5.0.2. Beaming breaks

The light curves of GRB afterglows often display jet breaks, attributed to the confinement of the relativistic outflow into a small cone. Rhoads (1997) has shown that jet breaks can be used to estimate θ_j , the jet opening angle, and E_γ , the total energy output in γ -rays. E_γ is given by the following formula

$$E_\gamma = E_{iso} * (1 - \cos(\theta_j))$$

where θ_j is the opening angle of the jet in radians.

The afterglows of GRB 020124 and GRB 030323 were observed on several occasions dur-

ing the few days following the bursts, but not frequently enough to unambiguously identify a possible jet break. Berger et al. (2002) nevertheless argue that GRB 020124 might have a jet break 10-20 days after the burst. The observations of GRB 030323, on the other hand, give an afterglow slope $s = -1.56 \pm 0.03$ (Vreeswijk et al. 2004), showing that they took place before a possible jet break (one expects $s \sim -2$ after the break). Fig.1. of Vreeswijk et al. (2004) shows that we can exclude a jet break in the afterglow, in the first 4 days following the burst.

Frail et al. (2001) find that E_γ is narrowly distributed around 5×10^{50} erg in a sample of GRBs with known redshifts. Bloom, Frail, and Kulkarni (2003) later revised this value to 1.3×10^{51} erg. From the measured value of E_{iso} , we can calculate the opening angle that the jet would have to have for E_γ to be 1.3×10^{51} erg. For GRB 020124, we find $\theta_j = 0.10$ radians (5.8 degrees), and $\theta_j = 0.29$ radians (16 degrees) for GRB 030323. Following equation (1) of Frail et al. (2001), and assuming a circumburst density of $[0.1 \text{ cm}^{-3}]$, we find that the expected break time is 2.6 days for GRB 020124, and 5.7 days for GRB 030323. With the freedom allowed by the poor sampling of the light curves, and by the small (but real) scatter in the size of the energy reservoir, we consider that these numbers do not contradict the finding of Frail et al. (2001), and Bloom, Frail, and Kulkarni (2003) that there is a standard radiated energy for GRBs.

5.0.3. *Host galaxy identification*

GRB 020124 and GRB 030323 have very faint hosts: $R \geq 29.5$ for GRB 020124 (Bloom et al. 2002), and $V=28.0$ for GRB 030323 (Vreeswijk et al. 2004). The early localization of these two GRBs, and the quick identification of their afterglows, made possible the identification of the host galaxy of GRB 030323, and placed stringent limits on the magnitude of the host galaxy of GRB 020124. The faintness of the host galaxies of these two bursts shows the impossibility to measure their redshifts from the spectroscopy of their host galaxies. GRB 020124 and GRB 030323 are examples of GRBs whose redshifts can only be measured at early times from the spectrum of the afterglow (unlike what was done for GRB 971214). The fact that two of the four GRBs known with $z \geq 3$ occurred in faint galaxies, may indicate that a non-negligible fraction of star formation takes place in such faint galaxies. Gamma-ray bursts appear to be a privileged way to identify this population.

6. Conclusions

This paper describes the temporal and spectral properties of GRB 020124 and GRB 030323, two GRBs at redshift $z > 3$ detected and localized with HETE. These two events are found to be fully consistent with the properties of the rest of the GRB population detected with HETE.

We have used the chain of events which successfully led to the measurement of the redshifts of GRB 020124 and GRB 030323 as a baseline to discuss the conditions required for the identification of high- z GRBs. Our two main conclusions are summarized below.

The fast localization of GRB 020124 and GRB 030323 allowed the quick identification and the early spectroscopy of their afterglows. We see a posteriori that this was the only way to measure their redshifts, given the faintness of their host galaxies. In these cases, contrary to the case of GRB 971214, we could not rely on the spectroscopy of the host galaxy to measure the redshifts, and this might well be the case for the majority of high- z GRBs.

Study of GRB 020124 shows that even instruments of modest size like FREGATE or the WXM are able to detect and localize GRBs up to $z=7-8$, if indeed GRBs occur at these redshifts. The study of the tracks with redshift of the peak flux and of the fluence of GRB 020124 provides insight into the strategy to be used for the detection of high- z GRBs. A strategy that relies mainly on the search for count excesses in short time intervals does not appear to be the most appropriate. A strategy based on the imaging of faint, soft transients lasting minutes appears more promising.

Acknowledgments

The HETE mission is supported in the U.S. by NASA contract NASW-4690; in Japan, in part by the Ministry of Education, Culture, Sports, Science, and Technology Grant-in-Aid 13440063; and in France, by CNES contract 793-01-8479. KH is grateful for HETE support under Contract MIT-SC-R-293291, for Ulysses support under JPL Contract 958056, and for IPN support under NASA grant FDNAG5-11451. G. Pizzichini acknowledges support by the Italian Space Agency.

REFERENCES

Amati, L., Frontera, F., Tavani, M., et al. 2002, *A&A*, 390, 81

- Andersen, M.I., Hjorth, J., Pedersen, H., et al. 2000, A&A, 364, L54
- Band, D., Matteson, J., Ford, L. et al. 1993, ApJ, 413, 281
- Barraud, C., Olive, J-F., Lestrade, J.P. et al. 2003, A&A, 400, 1021
- Barraud, C., Atteia, J-L., Olive, J-F. et al. 2004, AIP Conf. Proc. 727: Gamma-Ray Bursts: 30 Years of Discovery, 727, 81
- Berger, E., Kulkarni, S., Bloom, J. et al. 2002, ApJ, 581, 981
- Bloom, J.S., Berger, E., and Kulkarni, S.R. 2002, GCN Circ. 1452
- Bloom, J.S., Frail, D.A., and Kulkarni, S.R. 2003, ApJ, 594, 674
- Dal Fiume, D., Amati, L., Antonelli, L.A. et al. 2000, A&A, 355, 454
- Frail, D.A., Kulkarni, S.R., Sari, R. et al. 2001, ApJ, 562, L55
- Frontera, F., Amati, L., Costa, E. et al. 2000, ApJS, 127, 59
- Gilmore, A., Kilmartin, P., Henden, A. 2003, GCN Circ. 1949
- Graziani, C., Shirasaki, Y., Matsuoka, M. et al. 2003, GCN Circ. 1956
- Halpern, J.P., Thorstensen, J.R., Helfand, D.J., and Costa, E. 1998, Nature, 393, 41
- Hjorth, J., Møller, P., Gorosabel, J. et al. 2003, ApJ, 597, 699
- Hurley, K. et al. 2002, GCN Circ. 1223
- Kulkarni, S.R., Djorgovski, S.G., Ramaprakash, A.N., et al. 1998, Nature, 393, 35
- Lamb, D. Q., & Reichart, D. E. 2000, ApJ, 535, 1
- Lamb, D. Q., Sakamoto, T., Atteia, J-L. et al. 2005, ApJ, in preparation
- Preece, R. D., Briggs, M.S., Mallozzi, R.S. et al. 2000, ApJS126, 19
- Price, P.A., Fox, D.W., Yost, S.A. et al. 2002, GCN Circ. 1221
- Rhoads, J. 1997, ApJ, 487, L1
- Ricker, G.R., Atteia, J-L., Kawai, N. et al. 2002, GCN Circ. 1220
- Sakamoto, T., Lamb, D.Q., Suzuki, M. et al. 2004a, ApJ, 602, 875

Sakamoto, T., Lamb, D.Q., Graziani, C. et al. 2004b, ApJ, submitted (astro-ph/0409128)

Torii, K., Kato, T., Yamaoka, H. and Yoshida, A. 2002, GCN Circ. 1378

Vreeswijk, P., Ellison, S.L., Ledoux, C. et al. 2004, A&A, 419, 927

Table 1. Temporal Properties of GRB 020124 and GRB 030323.

GRB / Instrument	Energy (keV)	t_{90} (s)	t_{50} (s)
GRB 020124			
HETE WXM	2–25	50.2 ± 2.3	18.6 ± 1.1
	2–5	41.8 ± 0.4	23.5 ± 1.7
	5–10	50.4 ± 8.0	11.7 ± 3.0
	10–25	32.5 ± 1.2	16.7 ± 3.5
HETE FREGATE	6–400	49.4 ± 1.3	22.6 ± 1.0
	6–15	51.4 ± 1.4	26.0 ± 2.7
	15–30	52.9 ± 2.0	23.2 ± 2.4
	30–85	45.6 ± 0.7	22.2 ± 1.3
	85–400	43.0 ± 6.1	19.2 ± 1.8
GRB 030323			
HETE WXM	2–25	32.6 ± 2.7	13.9 ± 1.6
	2–5	31.5 ± 0.9	16.2 ± 0.8
	5–10	36.1 ± 0.6	19.4 ± 1.3
	10–25	19.5 ± 2.0	12.5 ± 1.3
HETE FREGATE	6–400	15.0 ± 2.6	7.1 ± 1.2
	6–30	12.8 ± 2.5	6.6 ± 1.5
	30–400	12.2 ± 3.6	5.2 ± 1.6

Note. — Errors are $1\text{-}\sigma$. The significantly longer duration measured by the WXM for GRB 030323 is explained by the better sensitivity of this instrument to low energy photons which are hardly detected with FREGATE.

Table 2. Spectral models for GRB020124 and GRB 030323. See section 3.2 for a description of the spectral models.

GRB / Model	Alpha	E ₀	Beta
GRB 020124 PLE	$-0.79^{+0.15}_{-0.14}$	87^{+34}_{-21}	N/A
GRB 020124 GRBM	$-0.87^{+0.16}_{-0.19}$	82^{+31}_{-31}	$-2.6_{-0.65}$
GRB 030323 PLE	$-0.80^{+0.8}_{-0.83}$	44^{+90}_{-26}	N/A
GRB 030323 GRBM ^a	$-0.96^{+1.31}_{-0.85}$	60_{-45}	-2.3 (frozen)

Note. — Errors are for 90% confidence, there is no upper limit for Beta. ^a For this model, the parameters are poorly constrained. β is frozen at -2.3 , and there is no upper limit on E₀.

Table 3. Emission Properties of GRB 020124 and GRB 030323.

Energy (keV)	Peak photon Flux (ph cm ⁻² s ⁻¹)	Peak energy Flux (erg cm ⁻² s ⁻¹)	Energy Fluence (erg cm ⁻²)
GRB 020124			
2–30	6.9 ± 1.6	$1.8 \pm 0.18 \times 10^{-7}$	$2.0^{+0.14}_{-0.14} \times 10^{-6}$
30–400	2.5 ± 0.40	$4.5 \pm 0.46 \times 10^{-7}$	$6.1^{+0.88}_{-0.76} \times 10^{-6}$
50–300	1.4 ± 0.28	$3.2 \pm 0.33 \times 10^{-7}$	$4.7^{+0.82}_{-0.82} \times 10^{-6}$
GRB 030323			
2–30	3.4 ± 2.1	$.57 \pm .16 \times 10^{-7}$	$3.4^{+1.3}_{-1.2} \times 10^{-7}$
30–400	0.49 ± 0.22	$1.5 \pm .43 \times 10^{-7}$	$8.9^{+3.8}_{-3.5} \times 10^{-7}$
50–300	0.29 ± 0.15	$1.0 \pm .29 \times 10^{-7}$	$6.5^{+2.8}_{-2.8} \times 10^{-7}$

Note. — Errors are given at the 90% confidence level.

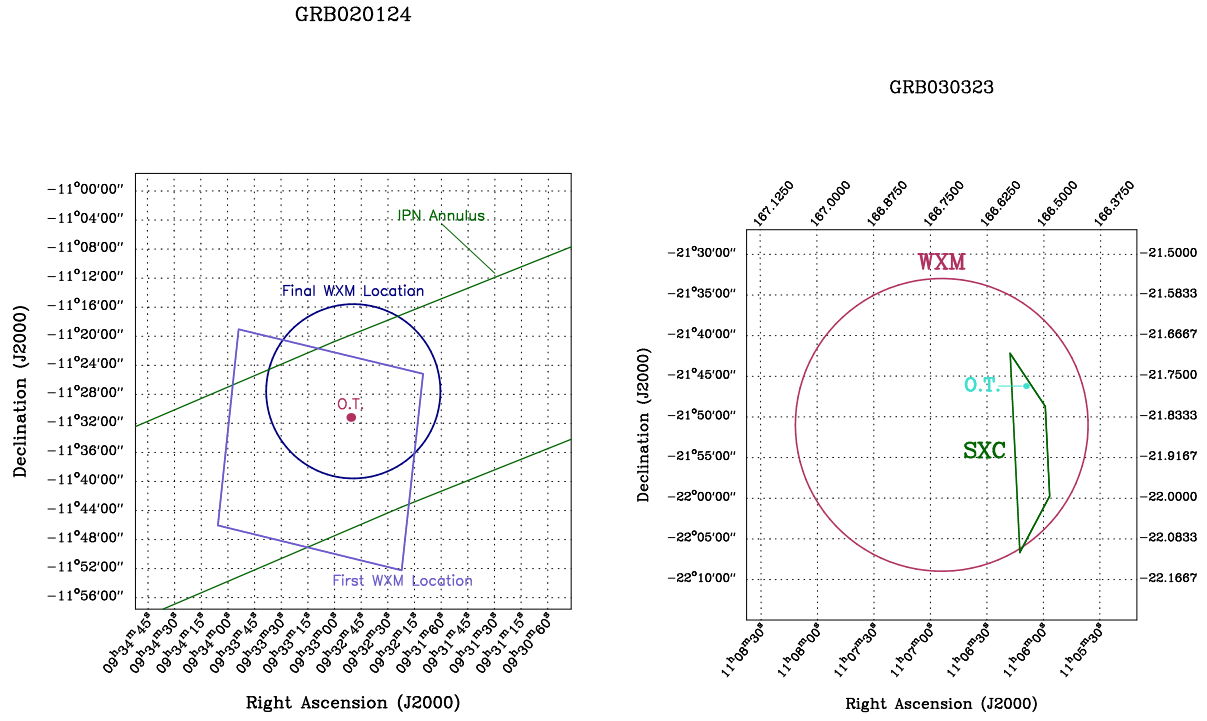


Fig. 1.— Left panel: Reported localizations and optical afterglow of GRB 020124. Right panel: Reported localizations and optical afterglow of GRB 030323.

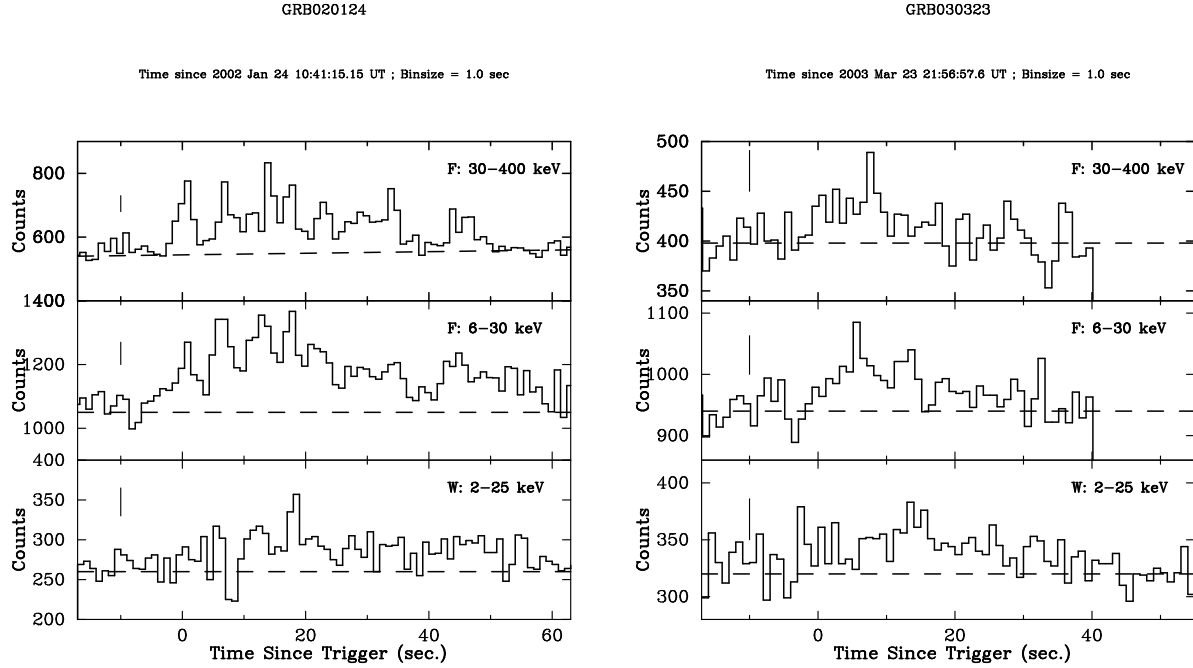


Fig. 2.— Left panel: Light curves of GRB 020124 in various energy bands. The lower panel shows the light curve recorded with the WXM (2-25 keV). The upper two panels show the light curves recorded with FREGATE in two energy bands (6-30 keV, and 30-400 keV). The vertical line at $t=-10$ sec shows the typical size of 1-sigma error bars. Right panel: Same plots for GRB 030323.

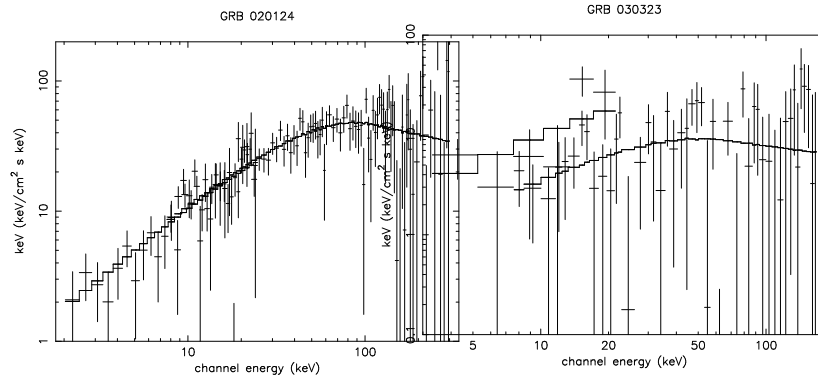


Fig. 3.— Left panel: Unfolded energy spectrum of GRB 020124 in the range 2-400 keV. Right panel: Unfolded energy spectrum of GRB 030323 in the range 2-400 keV.

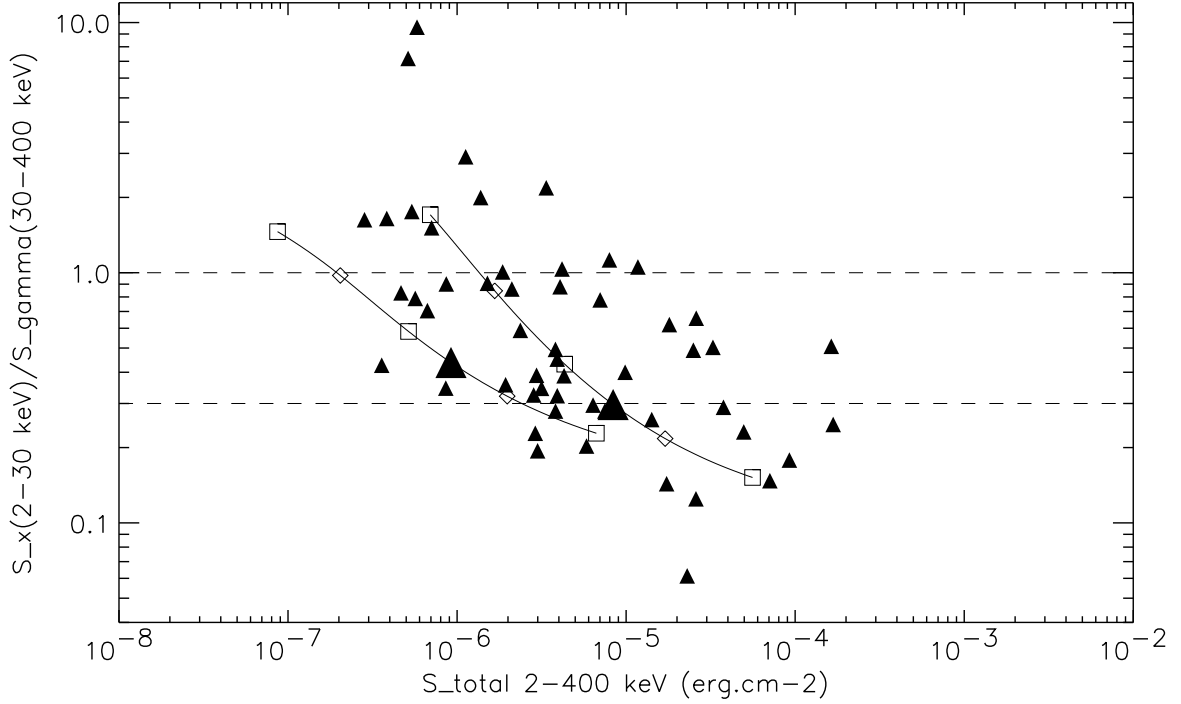


Fig. 4.— The position of GRB 020124 (rightmost large triangle) and GRB 030323 (leftmost large triangle) in a fluence-softness plot, among other GRBs detected with HETE (Barraud et al. 2004). The two solid lines show the tracks of GRB 020124 and GRB 030323 with redshift, from $z=1$ to $z=20$. Open squares indicate redshifts 1, 5 and 20 and open diamonds redshifts 2 and 10. This figure shows that at a redshift of unity GRB 020124 would have been in the bright end of the GRB fluence distribution, and GRB 030323 would have been in the middle of the distribution. This figure also shows that GRB 030323 is at the lower boundary of the fluence distribution of HETE GRBs, while GRB 020124 would still lie in the middle of this distribution, even at redshift $z \sim 10$. An estimate of the maximum redshift at which GRB 020124 could have been detected by HETE is given in section 4.1. The upper dashed horizontal line shows the boundary between X-Ray Flashes (above the line) and X-ray rich GRBs. The lower dashed horizontal line shows the boundary between X-ray rich GRBs and normal GRBs (below the line).